

(17)

Lasers
SLL 80 127/C/L
copy 17

Performance of XeF/KrF Lasers Pumped by Fast Discharge

Prepared by C. P. WANG
Aerophysics Laboratory

26 February 1976

Prepared for VICE PRESIDENT AND GENERAL MANAGER
LABORATORY OPERATIONS



Laboratory Operations
THE AEROSPACE CORPORATION

PLEASE RETURN TO:

BMD TECHNICAL INFORMATION CENTER
BALLISTIC MISSILE DEFENSE ORGANIZATION
7100 DEFENSE PENTAGON
WASHINGTON D.C. 20301-7100

19980309 289

U3997

DISTRIBUTION STATEMENT A

Approved for public release;
Distribution Unlimited

DTIC QUALITY INSPECTED 4

LABORATORY OPERATIONS

The Laboratory Operations of The Aerospace Corporation is conducting experimental and theoretical investigations necessary for the evaluation and application of scientific advances to new military concepts and systems. Versatility and flexibility have been developed to a high degree by the laboratory personnel in dealing with the many problems encountered in the nation's rapidly developing space and missile systems. Expertise in the latest scientific developments is vital to the accomplishment of tasks related to these problems. The laboratories that contribute to this research are:

Aerophysics Laboratory: Launch and reentry aerodynamics, heat transfer, reentry physics, chemical kinetics, structural mechanics, flight dynamics, atmospheric pollution, and high-power gas lasers.

Chemistry and Physics Laboratory: Atmospheric reactions and atmospheric optics, chemical reactions in polluted atmospheres, chemical reactions of excited species in rocket plumes, chemical thermodynamics, plasma and laser-induced reactions, laser chemistry, propulsion chemistry, space vacuum and radiation effects on materials, lubrication and surface phenomena, photosensitive materials and sensors, high precision laser ranging, and the application of physics and chemistry to problems of law enforcement and biomedicine.

Electronics Research Laboratory: Electromagnetic theory, devices, and propagation phenomena, including plasma electromagnetics; quantum electronics, lasers, and electro-optics; communication sciences, applied electronics, semiconducting, superconducting, and crystal device physics, optical and acoustical imaging; atmospheric pollution; millimeter wave and far-infrared technology.

Materials Sciences Laboratory: Development of new materials; metal matrix composites and new forms of carbon; test and evaluation of graphite and ceramics in reentry; spacecraft materials and electronic components in nuclear weapons environment; application of fracture mechanics to stress corrosion and fatigue-induced fractures in structural metals.

Space Sciences Laboratory: Atmospheric and ionospheric physics, radiation from the atmosphere, density and composition of the atmosphere, aurorae and airglow; magnetospheric physics, cosmic rays, generation and propagation of plasma waves in the magnetosphere; solar physics, studies of solar magnetic fields; space astronomy, x-ray astronomy; the effects of nuclear explosions, magnetic storms, and solar activity on the earth's atmosphere, ionosphere, and magnetosphere; the effects of optical, electromagnetic, and particulate radiations in space on space systems.

THE AEROSPACE CORPORATION
El Segundo, California

PERFORMANCE OF XeF/KrF LASERS
PUMPED BY FAST DISCHARGE

Prepared by
C. P. Wang
Aerophysics Laboratory

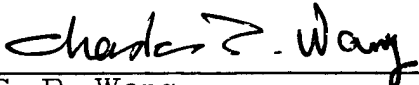
26 February 1976

Laboratory Operations
THE AEROSPACE CORPORATION
El Segundo, Calif. 90245

Prepared for
VICE PRESIDENT AND GENERAL MANAGER
LABORATORY OPERATIONS


PERFORMANCE OF XeF/KrF LASERS PUMPED
BY FAST DISCHARGE

Prepared




C. P. Wang

Approved



H. Mirels, Head
Aerodynamics and Heat Transfer
Department



W. R. Warren, Jr., Director
Aerophysics Laboratory

CONTENTS

ABSTRACT	vii
ACKNOWLEDGMENT	viii
I. INTRODUCTION	1
II. EXPERIMENTAL RESULTS	3
III. CONCLUSION	11
REFERENCES	13

FIGURES

1. Measured Output Energy vs Total Pressure for Various Kr and NF_3 Concentrations	4
2. Typical Output Pulse Shapes of KrF Laser at Various Energies	6
3. Measured Output Energy vs Total Pressure for Various Xe and NF_3 Concentrations	8
4. Typical Output Pulse Shapes of XeF Laser at Various Energies	10

ABSTRACT

The output energy and pulse shape of XeF/KrF lasers pumped by fast discharges were measured at various gas compositions and total pressures. For the KrF laser, the maximum output (1.6 mJ) was obtained in a gas mixture of He:Kr:NF₃ = 100:5:0.2 at a total pressure of 700 Torr. The output energy density was 160 mJ/l, and the wall-plug efficiency was 0.06%. The peak power was 55 kW. For the XeF laser, the maximum output (10 mJ) was obtained in a gas mixture of He:Xe:NF₃ = 100:4:2 at a total pressure of 500 Torr. The peak output power was 1 MW. The output energy density (660 mJ/l) was a factor of 10 higher, and the wall-plug efficiency (0.5%) was a factor of 2.5 higher than reported earlier.

ACKNOWLEDGMENT

The author is indebted to Harold Mirels for many helpful discussions, and O. L. Gibb for technical assistance.

I. INTRODUCTION

The rare gas monohalide lasers are a new class of efficient, high-power lasers operating in the ultraviolet. The laser action has been predicted and subsequently demonstrated by direct electron-beam excitation,¹⁻⁵ electron-beam-controlled discharge excitation,⁶ and fast-discharge excitation.⁷⁻⁹ Lasers in XeF with wavelengths of 351, 353, and 349 nm and in KrF with wavelengths of 249 and 250 nm have produced the greatest powers and efficiencies. The performance of these lasers, however, is still far from optimum because the excitation mechanism, gas kinetics, fast discharge, and plasma stability are not well understood. The operating conditions, such as total gas pressure, species concentration, and discharge (or electron-beam) voltage and current have not yet been optimized.

Since the demonstration of laser action by a fast-discharge device¹⁰ in XeF⁸ and in KrF,⁹ an order of magnitude improvement in laser performance has been achieved by systematically varying the gas pressure, gas composition, discharge voltage and current, and line impedance. Preliminary results are reported here on the output energy and pulse shape of fast-discharge-initiated XeF/KrF lasers as functions of total gas pressure and gas composition. The significance of this study is that optimum gas compositions and pressures as well as the general behavior of the laser performance are obtained for several voltage levels. Also, data are provided for the theoretical modeling of XeF/KrF laser performance.

II. EXPERIMENTAL RESULTS

The construction and discharge characteristics of the fast-discharge device have been described earlier.¹⁰ Briefly, it is a Blumlein-type fast-discharge device with a discharge duration of 10 nsec. The width of the line (50 cm), the length of the line (100 cm), and the height of the electrode (0.33 cm) are all fixed. The electrode separation, however, can be varied from 0.5 to 2 cm; the line impedance can be varied from 0.04 to 0.20 ohms; the discharge voltage can be varied from 5 to 20 kV; and the gas pressure can be varied from 20 to 700 Torr. The most important features of this fast-discharge device are: fast rise time, variable line impedance and electrode separation, and the capability to operate at high pressures without excessive arcing.

The laser output energy was measured with a Molectron joulemeter (Model J3-05) with fine-mesh screen attenuators. The laser output pulse shape was monitored with an ITL fast vacuum-photodiode (100 psec rise time) and a Tektronix 7844 oscilloscope with a 7A12 plug-in unit. The output wavelengths were measured with a Jarrell-Ash 1/2 m grating spectrograph.

For the KrF laser, a discharge volume of $0.6 \times 0.33 \times 50 \text{ cm} = 10 \text{ cm}^3$ and line impedance of 0.05 ohm were used. The discharge voltage was 8 kV. The laser cavity was a 4 m radius-of-curvature dielectrically coated total reflector with 98.5% reflectivity and a flat dielectrically coated output mirror with 95% reflectivity. The separation between mirrors was 90 cm. These mirrors were mounted internally, without Brewster windows, in order to reduce losses. The measured output wavelengths were 248.5 and 249.5 nm.

Gas mixtures of He, 5-20% Kr, and 0.2-0.4% NF_3 were used at total pressures of 200-700 Torr. The measured output energy versus total pressure for various concentration of Kr and NF_3 is plotted in Fig. 1. Each measurement was obtained by averaging over more than ten pulses at a pulse repetition rate of 1 Hz. With a single filling of gas mixture, several hundred laser pulses can be obtained with little or no degradation of output energy.

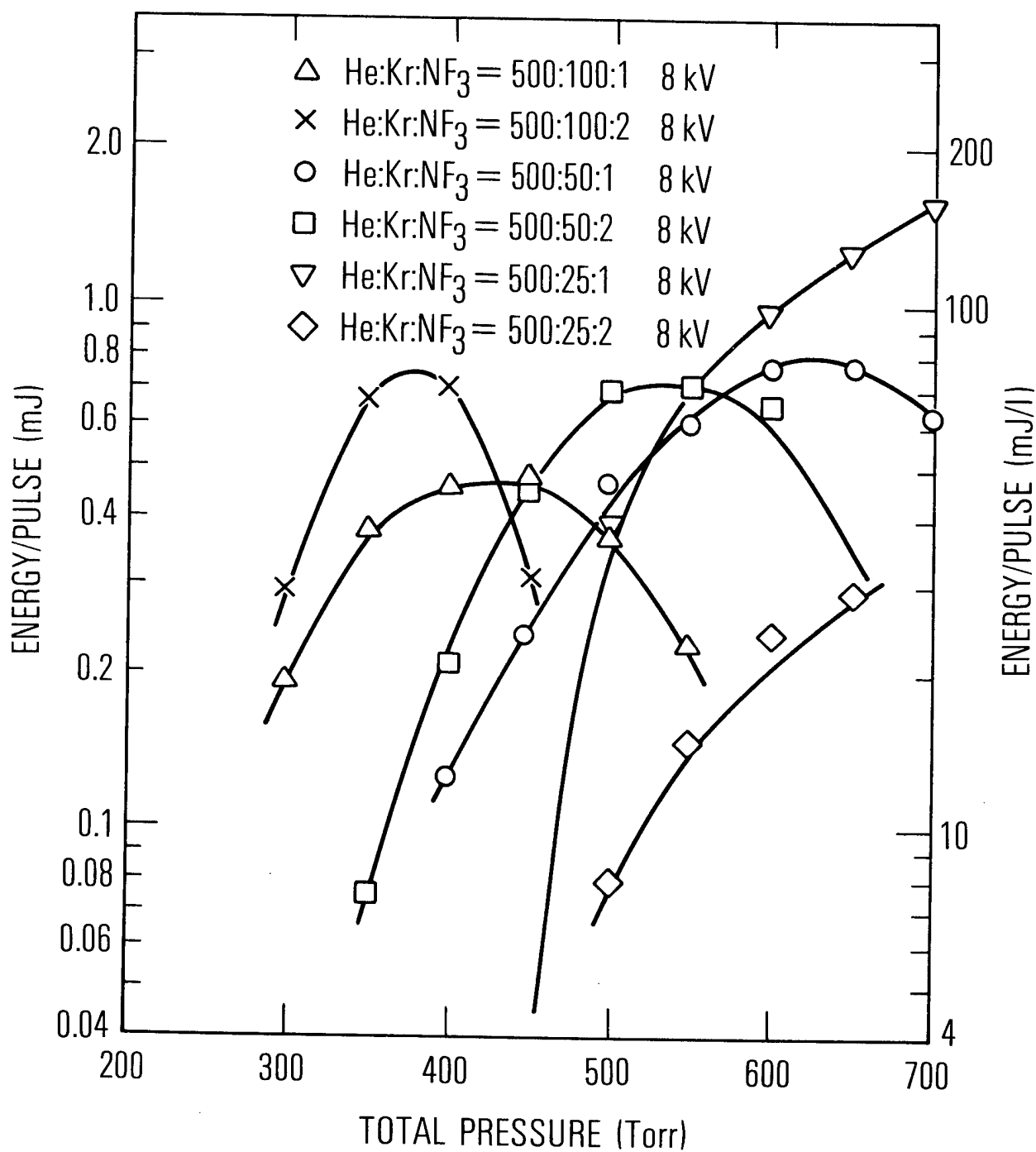


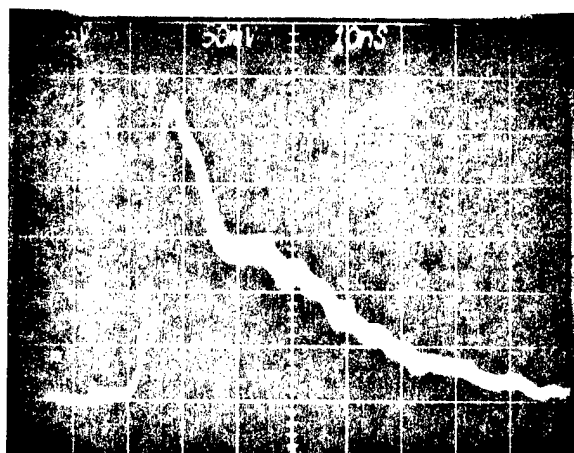
Figure 1. Measured Output Energy vs Total Pressure for Various Kr and NF₃ Concentrations

The experimental result (Fig. 1) shows that, for high Kr concentrations ($\text{He/Kr} = 5/1$), laser action starts at relatively low pressure (250 Torr), and the output energy then reaches a maximum near 400 Torr for 0.4% NF_3 and near 450 Torr for 0.2% NF_3 . For lower Kr concentrations ($\text{He/Kr} = 10/1$), laser action starts near 350 Torr, and the output energy then reaches a maximum near 500 Torr for 0.4% NF_3 and near 600 Torr for 0.2% NF_3 . The peak output energy is slightly higher than that obtained in the high-Kr concentration mixtures. With further decreases in Kr concentration ($\text{He/Kr} = 20/1$), laser action starts near 450 Torr, and the output energy continuously increases up to 700 Torr without reaching a maximum. In the present tests, the highest output energy (1.6 mJ) was obtained in a mixture of $\text{He:Kr:NF}_3 = 100:5:0.2$ at a total pressure of 700 Torr. The output energy density was 160 mJ/l, and the wall-plug efficiency was 0.06%.

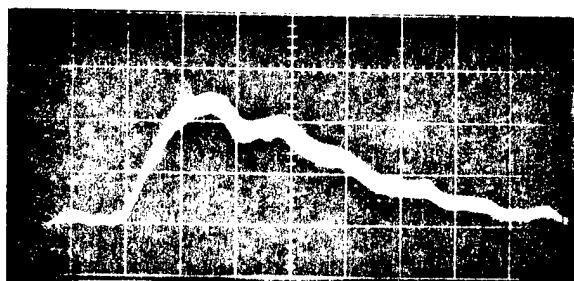
It appears that the saturation or decrease of output energy at higher total pressure for $\text{He/Kr} = 5/1$ and $10/1$ is due to excessive arc formation. As for the effects of NF_3 , it appears that the higher concentration of NF_3 quenches the excited KrF^* molecule. It is the delicate balance between the rate of formation of KrF^* and the rate of quenching of KrF^* by NF_3 that determines the optimum ratio of Kr and NF_3 .

The measured laser pulse shapes at various output energies are shown in Fig. 2. Each photograph is a multiple exposure of ten shots. At low energy, the output pulse shape appears to consist of two overlapping pulses of approximately equal amplitude. The pulse width (FWHM) is about 30 nsec (Figs. 2b and 2c). At higher output energy, the amplitude of the first pulse increased much more than the second pulse (Fig. 2a). The first pulse appears to be dominant. Its pulse width is about 10 nsec. In as much as the discharge duration is about 10 nsec, the first pulse must occur during discharge, whereas the second occurs in the afterglow. Similar behavior was noted in the XeF laser discussed below.

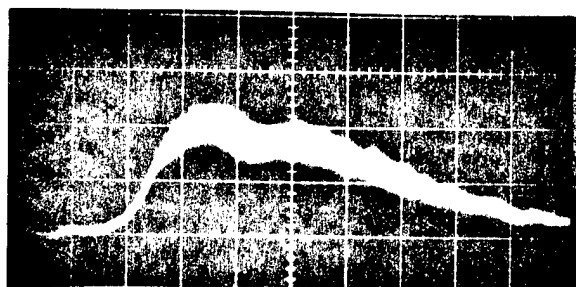
For the XeF laser, a discharge volume of $0.9 \times 0.33 \times 50 \text{ cm} = 15 \text{ cm}^3$ and line impedance of 0.04 ohm were used. The discharge voltage was 7 kV.



a



b



c

Figure 2. Typical Output Pulse Shapes of KrF Laser at Various Energies. a. 1.6 mJ, 10 kW/div; b. 0.8 mJ, 10 kW/div; c. 0.2 mJ, 2.5 kW/div. Sweep speed, 10 nsec/div.

The laser cavity was a 10 m radius-of-curvature dielectrically coated total reflector with reflectivity greater than 97% and a flat dielectrically coated output mirror with 80% reflectivity. The separation between mirrors was 90 cm. The measured output wavelengths were 353, 351, and 349 nm.

Gas mixtures of He, 3-10% Xe, and 0.5-2.0% NF_3 were used at total pressures of 200-700 Torr. The measured output energy versus total pressure at various concentrations of Xe and NF_3 is plotted in Fig. 3. Each measurement was obtained by averaging over more than ten pulses. The output energy is shown to depend on the mole fraction of Xe and NF_3 as well as total gas pressure. This is contrary to the results of Burnham, Harris, and Djeu,⁷ where the output energy depended only on the mole fraction of Xe and NF_3 . The general pattern is similar to the case of the KrF laser. However, both the output energies and the NF_3 concentrations are an order of magnitude higher than in the KrF laser. The higher concentration of NF_3 used in the XeF laser indicates that concentrations of NF_3 up to 2% do not significantly change the discharge characteristics or cause excessive arcing. The use of low ratios of Xe/ NF_3 indicates that the quenching of XeF^* by NF_3 is insignificant. This confirms the assumption used in Ref. 8.

The Xe concentration used here was much higher than that reported by Burnham, Harris, and Djeu⁷ since the fast-discharge device used here, because of its short discharge time, low line impedance, and electrode geometry, can operate at relatively high Xe concentrations without excessive arcing.

The optimum gas composition was found to be $\text{He:Xe:NF}_3 = 100:4:2$. At the highest discharge voltage (9 kV), a maximum output of 10 mJ was obtained at 500 Torr. The peak output power was 1 MW. The maximum output energy density was 660 mJ/l, and the wall-plug efficiency was 0.5%. Compared with the results obtained previously,⁸ output energy density of 70 mJ/l and wall-plug efficiency of 0.2%, the present results are an order of magnitude improvement in output energy density and a factor of 2.5 improvement in efficiency. Further improvement is possible with different gas additives, higher discharge voltages, and better impedance matching.

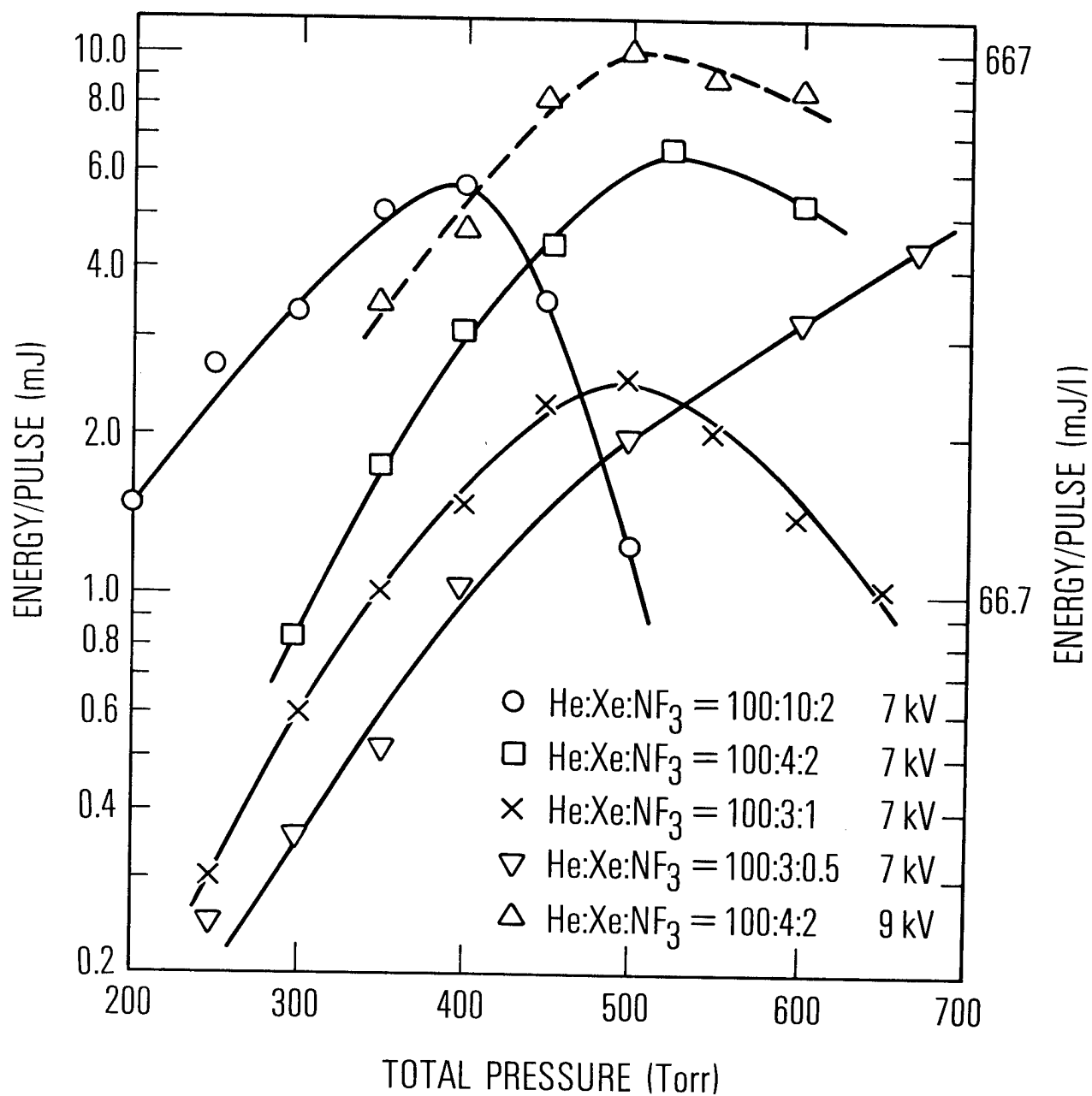
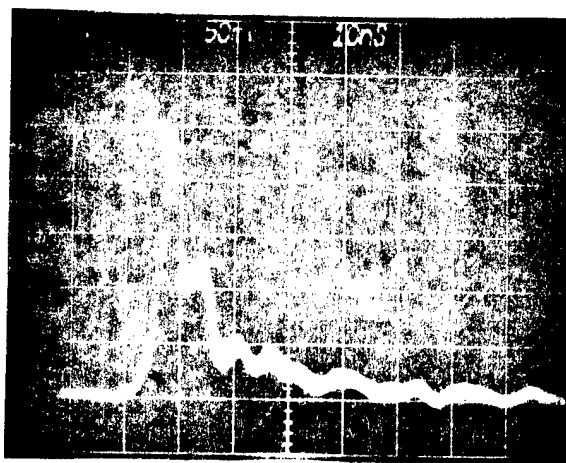


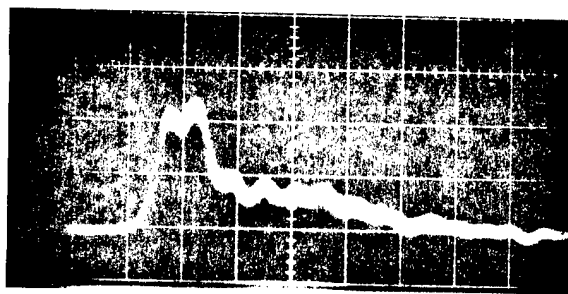
Figure 3. Measured Output Energy vs Total Pressure for Various Xe and NF₃ Concentrations

The Fresnel number of the cavity is relatively high, and the laser output beam contains higher-order modes. The typical output beam cross section is 0.6×0.4 cm near the output mirror, and the beam divergence is much less than 1 mrad. This is much better than in the N_2 laser, which is operated at superradiance mode.

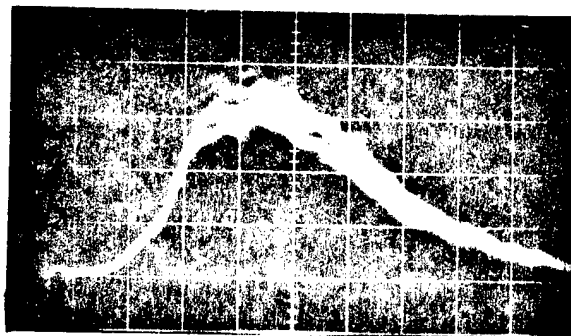
Typical XeF laser pulse shapes at various output energies are shown in Fig. 4. Each photograph is a multiple exposure of ten pulses. At low energy, the pulse width (FWHM) is about 40 nsec (Fig. 4c). As the output energy is increased, a sharp peak develops and the pulse width decreases. The pulse width decreased to about 12 nsec at 2.5 mJ output (Fig. 4b) and about 6 nsec at 10 mJ output (Fig. 4a). The two-overlapping-pulses feature discussed earlier is also evident in Figs. 4a and 4b.



a



b



c

Figure 4. Typical Output Pulse Shapes of XeF Laser at Various Energies.
 a. 10 mJ, 200 kW/div; b. 2.3 mJ, 50 kW/div; c. 0.3 mJ, 1.5 kW/div.
 Sweep speed, 10 nsec/div.

III. CONCLUSION

An order of magnitude improvement has been achieved in XeF/KrF laser output by optimizing gas composition, total pressure, and line impedance. Further improvement is possible as the excitation mechanism, gas kinetics, plasma stability, and fast discharges are better understood. The effect of various discharge voltages will be investigated in a later study.

REFERENCES

1. J. E. Velazco and D. W. Setser, J. Chem. Phys. 62, 1990 (1975).
2. J. J. Ewing and C. A. Brau, Appl. Phys. Lett. 27, 350 (1975).
3. C. A. Brau and J. J. Ewing, Appl. Phys. Lett. 27, 435 (1975).
4. E. R. Ault, R. S. Bradford, Jr., and M. L. Bhaumik, Appl. Phys. Lett. 27, 413 (1975).
5. M. L. Bhaumik, R. S. Bradford, Jr., and E. R. Ault, Appl. Phys. Lett. 28, 23 (1976).
6. J. A. Mangano and J. H. Jacob, Appl. Phys. Lett. 27, 495 (1975).
7. R. Burnham, N. W. Harris, and N. Djeu, Appl. Phys. Lett. 28, 86 (1976).
8. C. P. Wang, H. Mirels, D. G. Sutton, and S. N. Suchard, Appl. Phys. Lett. (to be published).
9. D. G. Sutton, S. N. Suchard, O. L. Gibb, and C. P. Wang, Appl. Phys. Lett. (to be published).
10. C. P. Wang, Rev. Sci. Instrum. 47, 92 (1976).

DISTRIBUTION

Internal

J. F. Bott	S. W. Mayer
G. A. Capelle	R. X. Meyer
R. A. Chodzko	G. P. Millburn
N. Cohen	H. Mirels
E. G. Cross	V. H. Monteil
P. M. Diamond	A. H. Silver
D. A. Durran	S. N. Suchard
J. W. Ellinwood	D. J. Sutton
M. Epstein	D. J. Spencer
R. R. Giedt	B. L. Taylor
W. A. Griesser	T. D. Taylor
R. W. F. Gross	E. B. Turner
R. A. Hartunian	R. H. Ueunten
R. F. Heidner	R. L. Varwig
J. M. Herbelin	C. P. Wang
R. Hofland, Jr.	W. R. Warren, Jr.
J. J. Hough	K. R. Westberg
G. W. King	R. L. Wilkins
M. A. Kwok	

External

SAMSO

Lt. Col. Staubs (DYN)
Lt. Col. J. R. Doughty (DYV)

AFWL

Kirtland AFB, NM 87117
Col. R. Rose (AL)
Dr. P. Avizonis (AR)
Lt. Col. G. D. Brabson (ALC)
Lt. Col. M. Bina (ALC)
Maj. C. Forbrich (ALC)
Dr. L. Wilson (ALC)
Maj. D. Mitchell (DYT)

ARPA
1400 Wilson Blvd.
Arlington, VA 22209
Dr. P. Clark
R. A. Moore

AFRPL
Edwards AFB
Edwards, CA 93523
B. R. Bornhorst (LKCG)

Naval Research Laboratory
Code 5503, LTPO
Washington, DC 20390
Dr. W. Watt
Dr. R. Airey
Dr. J. M. MacCallum

Deputy Chief of Staff for Research,
Development and Acquisition
Dept. of the Army, Headquarters
The Pentagon
Washington, DC 20310
Lt. Col. Benjamin J. Pellegrini/
3B482

Los Alamos Scientific Laboratory
Los Alamos, NM 87544
Dr. K. Boyer
Dr. R. Jensen
Dr. G. Schott
Dr. J. Parker
Dr. E. Brock

AMSMI-RK
Redstone Arsenal, AL 35809
Dr. W. B. Evers, AMSMI/RK
Dr. J. Hammond, AMSMI/RK
Dr. W. Wharton, Bldg. 5452/RKL

AMSMI-RRP
Bldg. 4762
Redstone Arsenal, AL 35809
Dr. T. A. Barr, Jr.

U.S. Naval Ordnance Lab
Silver Spring, MD 20910
Dr. L. Harris
Dr. D. Finkleman

NASA Ames Research Center
Moffett Field, CA 94035
Dr. C. F. Hansen
Dr. H. Mark

Lawrence Radiation Lab
Livermore, CA 94550
Dr. A. Karo
Dr. J. Emmett

Arnold Engineering Development
Center
Arnold Air Force Station, TN 37389
Lt. R. Case (XOOE)

AFWAL
Wright-Patterson AFB, OH 45433
Dr. K. Scheller
Dr. J. Drewry

ESD (TRI)
L. G. Hanscom AFB, MA 01731

AFCRL (OPL)
Cambridge Research Laboratory
Hanscom Air Force Base, MA 01730
Dr. H. Schlossberg

AFSC (DLS)
Andrews AFB
Washington, DC 20331

AFML (SU)
Wright-Patterson AFB, OH 45433

AFAL (CA)
Wright-Patterson AFB, OH 45433
Dr. B. List

Air University Library
Maxwell AFB, AL 36112

Air Force Office of Scientific Research
Bolling AFB, Bldg. 410
Washington DC 20332
Directorate of Aerospace Sciences
Directorate of Physics

FJSRL (Tech Library)
USAF Academy
Colorado 80840

Scientific and Technical Info.
Facility (UNC)
P.O. Box 33
College Park, MD 20740 (A-Only)
NASA Representative

RADC (SU)
Griffiss AFB, NY 13442

NASA-Lewis Research Center
21000 Brookpark Road
Cleveland, OH 44135
S. Cohen/M.S. 500-209

DDR&E
Space Technology
The Pentagon 3E139
Washington, DC 20301
Dr. R. A. Greenberg, Asst. Director

U.S. Army
Advanced Missile Defense Agency
1300 Wilson Blvd.
Arlington, VA 22209
Dr. M. Zlotnick, RDMD-NC
Dr. L. Stoessell

U.S. Atomic Energy Commission
Division of Military Applications
Energy Resources Development Agency
Washington, DC 20301
Dr. George W. Rhodes
Dr. James McNally

Commander
Naval Weapons Center
China Lake, CA 93555
Eric Lundstrom/Code 4011

TRW Systems Group
One Space Park
Redondo Beach, CA 90278
Dr. T. A. Jacobs
Dr. G. Emanuel
Dr. J. Miller 01/1080

CALSPAN Corporation
P.O. Box 235
Buffalo, NY 14221
Dr. J. Daiber
Dr. E. C. Treanor

Martin-Marietta
Denver, CO 80202
Dr. J. Bunting

Rocketdyne
Canoga Park, CA 91304
Dr. S. V. Gunn
Dr. M. Constitine

Cornell University
Dept. of Thermal Engineering and
Lab. of Plasma Physics
Ithaca, NY 14853
Dr. T. A. Cool

Lockheed Palo Alto Research Lab
Palo Alto, CA 94304
Dr. W. C. Marlow

Lockheed Missiles and Space Company
4800 Bradford Blvd.
Huntsville, AL 35812
J. W. Benefield

McDonnell Research Laboratory
McDonnell Douglas Corporation
St. Louis, MO 63166
Dr. D. P. Ames
Dr. R. Haakinen

Physics International Company
2700 Merced Street
San Leandro, CA 94577
Dr. B. Bernstein

Massachusetts Institute of Technology
Department of Physics
Cambridge, MA 02139
Dr. A. Javan

Mathematical Sciences Northwest, Inc.
2755 Northrup Way
Bellevue, WA 98004
Dr. S. Byron
Prof. A. Hertzberg

McDonnell Douglas
5301 Bolsa Ave.
Huntington Beach, CA 92647
Dr. R. Lee/Bldg. 28, Rm. 250
Dr. G. Berend/Bldg. 28, Rm. 250
Dr. W. A. Gaubatz

United Technologies Research
Laboratories
400 Main Street
East Hartford, CT 06108
Dr. D. Seery
Dr. C. Ultee
Dr. G. H. McLafferty

Hughes Research Laboratory
3011 Malibu Canyon Road
Malibu, CA 90265
Dr. A. Chester

Avco-Everett Research Lab
2385 Revere Beach Parkway
Dr. G. W. Sutton
Dr. J. Dougherty

Columbia University
Dept. of Chemistry
New York, NY 10027
Dr. R. Zare

Science Applications, Inc.
P.O. Box 328
5 Research Drive
Ann Arbor, MI 48105
Dr. R. E. Meredith

Bell Aerosystems Company
P.O. Box 1
Buffalo, NY 14240
Dr. W. Solomon

Northrop Corporation Laboratories
Hawthorne, CA 90250
Dr. M. L. Bhaumik

The RAND Corporation
Via: AF Contracting Officer
1700 Main Street
Santa Monica, CA 90406
Library - 98D
for Dr. H. Watanabe

General Electric Company
U7211 VFSTC
P.O. Box 8555
Philadelphia, PA 19101
R. Geiger

Lockheed Missiles and Space Company
P.O. Box 1103, West Station
Huntsville, AL 35807
Dr. S. C. Kurzius

Princeton University
Dept. of Aerospace and Mech. Science
Princeton, N. J.
Prof. S. Bogdonoff

Purdue University
School of Mechanical Engineering
Chaffee Hall
Lafayette, IN 47907
Prof. J. G. Skifstad

California Institute of Technology
Pasadena, CA 91109
Dr. A. Kuppermann
Dr. H. Liepmann

University of Maryland
College Park, MD 20740
Dr. J. D. Anderson, Jr.
Head, Dept. of Aerospace
Engineering
College of Engineering

Perkin-Elmer Corporation
Norwalk, CA 06856
M. L. Skolnick
Electro-Optical Division

Dr. Walter R. Sooy
SAI
1651 Old Meadow Road
McLean, VA 222101